WATER RESOURCES RESEARCH, VOL. 28, NO. 9, PAGES 2211–2227, SEPTEMBER 1992

# Simulation of Dispersion in Heterogeneous Porous Formations: Statistics, First-Order Theories, Convergence of Computations

ALBERTO BELLIN

*Dipartimento di Ingegneria Civile ed Ambientale, Università di Trento, Trent, Italy*

PAOLO SALANDIN

*Istituto di Idraulica "Giovanni Poleni," Università di Padova, Padua, Italy*

ANDREA RINALDO

*Dipartimento di Ingegneria Civile ed Ambientale, Università di Trento, Trent, Italy*

This paper discusses the results of numerical analysis of dispersion of passive solutes in two-dimensional heterogeneous porous formations. Statistics of flow and transport variables, the accuracy and the role of approximations implicit in existing first-order theories, and the convergence of computational results are investigated. The results suggest that quite different rates of convergence with Monte Carlo runs hold for different spatial moments and that over 1000 realizations are required to stabilize second moments even for relatively mild heterogeneity ($\sigma_Y^2 < 1.6$). This has implications for the extent of the spatial domain for single-realization numerical studies of the same type. A comparison of the variance of plumes with the results of linear theories ($0.05 < \sigma_Y^2 < 1.6$) shows an unexpectedly broad validity field for the theoretical solution obtained from a suitable linearization of flow and transport. Reformulation of the same problem linearizing in turn the flow or the transport equations shows opposite deviations from the linear theory. The interesting consequence is that the errors induced by linearizations in the flow or the transport equations have different signs, and their effects on the moments of dispersing plumes are compensating, thereby yielding consistent formulations. Unexpected features of the statistics of probability distributions of longitudinal and transverse velocities and travel times are also computed and discussed.

## 1. INTRODUCTION

This paper discusses numerical simulations of dispersion of passive solutes in heterogeneous porous formations. Its aims are the discussion of a methodology for the assessment of convergence of computations; the study of statistics of flow and transport variables; and the study of the individual role and the mutual interactions of the approximations implicit in existing first-order theories.

Recent experimental evidence and theoretical results suggest that the transport of passive solutes in natural porous formations is dominated by the spatial variations in hydraulic conductivity resulting in heterogeneous convection fields (see, for an exhaustive review, *Dagan* [1989]). A theory of flow and transport has been developing in recent years [*Gelhar and Axness*, 1983; *Dagan*, 1984, 1987, 1988, 1989, 1990; *Gelhar*, 1986; *Neuman et al.*, 1987; *Barry et al.*, 1988; *Neuman and Zhang*, 1990] which links the kinematics of the dispersion process to field measurable quantities, i.e., the spatial correlation structure and the variability of the log conductivity field $Y(\mathbf{x})$ of porous formations viewed as a random space function. Fundamental experimental validations from accurate field analyses and critical elaborations of the data support the validity of linear theories at least for mildly heterogeneous aquifers [e.g., *Freyberg*, 1986; *Mackay et al.*, 1986; *Sudicky*, 1986; *Woodbury and Sudicky*, 1991; *Barry et al.*, 1988; *Naff et al.*, 1988; *Graham and McLaughlin*, 1991; *Le Blanc et al.*, 1991, *Garabedian et al.*, 1991; *Rajaram and Gelhar*, 1991].



Paper number 92WR00578.
0043-1397/92/92WR-00578$05.00

Limits and validity of the theory of flow and transport in heterogeneous porous formations have recently been discussed [*Dagan*, 1989]. It is accepted that the linear (denoted here as Dagan's) theory subsumes a number of previous results [*Matheron and de Marsily*, 1980; *Dagan*, 1984; *Gelhar and Axness*, 1983; *Dagan*, 1987] and captures the foremost features of the processes whenever the variance of log conductivity $\sigma_Y^2$, a significant measure of heterogeneity, is small ($\sigma_Y^2 < 1$) because a first-order perturbation is used as a consistent approximation involving such a parameter.

Implicit in the reference theory are the following assumptions [*Dagan*, 1987]: (1) Lagrangian and Eulerian statistical stationarity and homogeneity; (2) linearized statistics of the convection field, i.e., deduced from the linearized flow equation; and (3) negligible fluctuations of particles' displacements about the mean trajectory. Alternatively, Corrsin's conjecture has been assumed, yielding an explicit dependence of the moment equations on the covariance of velocities.

The relative role and the mutual interactions of nonlinear terms neglected in the formulation of first-order theories for increasingly heterogeneous conductivity fields have been the subject of a number of numerical and theoretical investigations. Most notable among the latter are recent contributions which attempt to capture the effects of nonlinear terms related to deviations from the average trajectory of particles by relaxing assumption 3 according to an iterative scheme [*Neuman and Zhang*, 1990; *Zhang and Neuman*, 1990] or

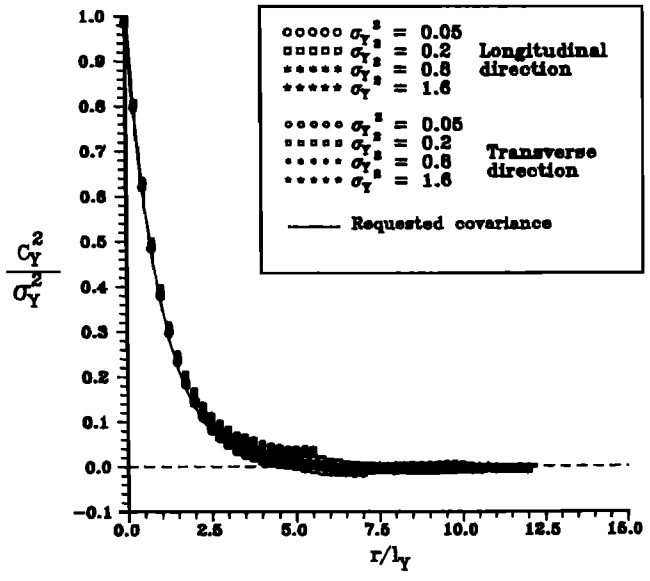


Fig. 1. Covariances of numerically reconstructed log conductivity fields $Y$.

numerically [*Rubin*, 1990]. Accuracy and convergence of computations, and flow and transport statistics are also investigated in this paper.

This study uses numerical tools involving numerical flow field solution and particle-tracking techniques following a significant body of literature [e.g., *Freeze*, 1975; *Smith and Freeze*, 1979; *Smith and Schwartz*, 1980, 1981; *Ababou et al.*, 1989; *Rubin*, 1990; *Salandin and Rinaldo*, 1990; *Salandin*, 1990; *Tompson et al.*, 1989; *Valocchi*, 1990; *Russo*, 1991]. The numerical analysis consists of (1) efficient generation of single realizations of random transmissivity fields with a specified spatial correlation structure; (2) suitably accurate finite element solution of the flow field for every realization; (3) particle-tracking techniques (unaffected by boundary effects) for the solution of the transport equation; (4) Monte Carlo iterations for steps 1–3; and (5) ensemble averaging. The foremost numerical problems in this context concern the amount of computation required to establish accuracy and convergence. Two lines of thought are currently being followed in the literature. The former employs a large single-realization domain, postulating that a sufficient number of uncorrelated particles can be released in the direction transverse to the flow to yield reliable ensemble averaging [*Ababou et al.*, 1989; *Tompson et al.*, 1989; *Valocchi*, 1990]. The latter iterates flow realizations in a Monte Carlo manner, producing several independent random fields of transmissivity with a specified spatial correlation structure, solving flow and transport for each of them and averaging over the different realizations [*Freeze*, 1975; *Smith and Freeze*, 1979; *Smith and Schwartz*, 1980, 1981; *Salandin*, 1990; *Salandin and Rinaldo*, 1990; *Salandin et al.*, 1991]. Both techniques require extensive use of computations and pose serious theoretical and numerical problems as the measure of heterogeneity grows large. The second path is pursued in this paper because of its flexibility in ascertaining convergence of computations.

To investigate the relative role of the linearization of flow and transport, the problem has also been reformulated in what might be called an inconsistent manner, i.e., linearizing the flow or the transport equations independently. Flow linearization has already been assumed to test the validity of linear theories [*Rubin*, 1990]. In fact, particle-tracking techniques are a viable and efficient tool for nonlinear transport and an analytical solution of a general nature is available for the statistical structure of the linear velocity field [*Neuman et al.*, 1987; *Dagan*, 1987].

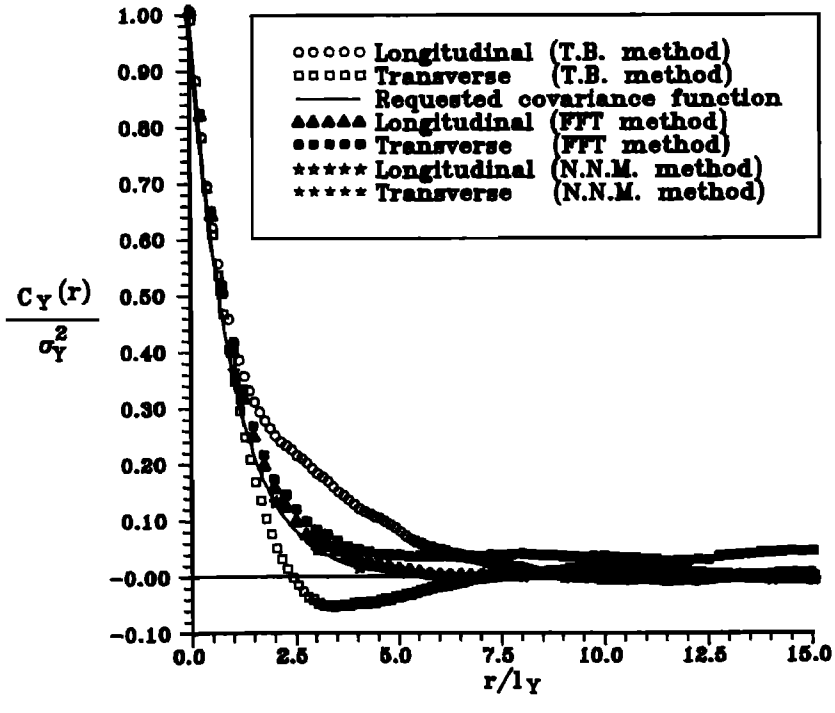


Fig. 2. A comparison of the performance of FFT-based, matrix (NNM) and turning bands (TB) methods for the generation of random lognormal fields with assigned spatial correlation structure.

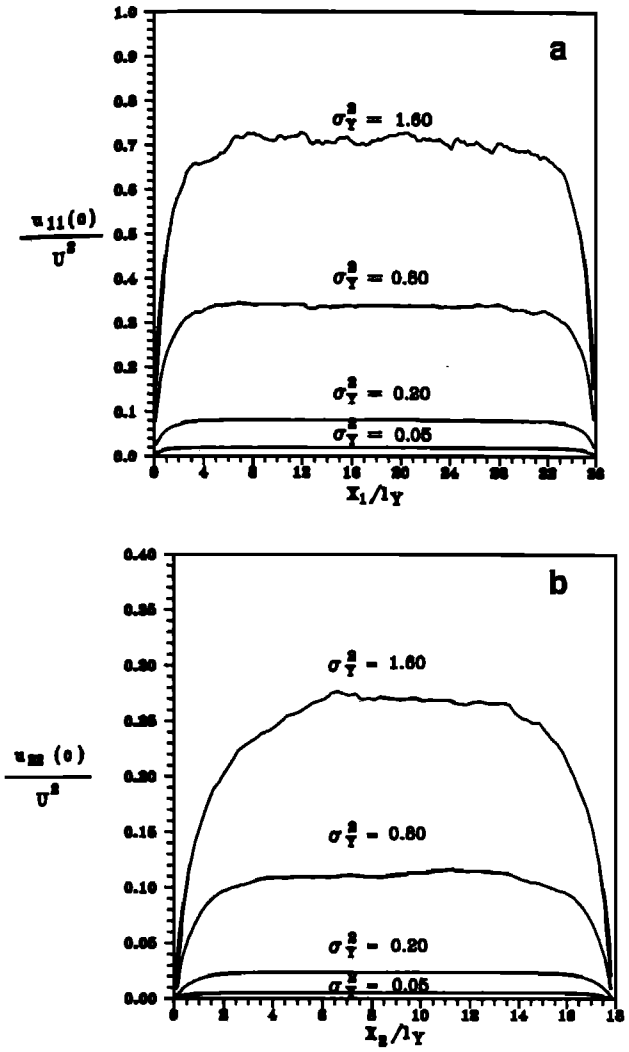


Fig. 3. Computed (*a*) longitudinal and (*b*) transverse velocity variances $u_{11}(0)$ and $u_{22}(0)$ versus Cartesian coordinates along the flow domain for several values of $\sigma_Y^2$.

The plan of the paper is as follows. Section 2 describes the numerical procedures related to the generation of two-dimensional random fields with preset spatial correlation structure and the finite element and particle-tracking schemes adopted. Section 3 presents computational results related to accuracy and convergence of numerical results and of statistics. This section is mostly devoted to the methodology adopted for ascertaining the reliability of the results. Section 4 discusses the results of extended statistics on flow and transport variables. Section 5 describes comparisons of computational results with linear theories and with partially linearized models of the same processes in the range $0.05 < \sigma_Y^2 < 1.6$. A set of conclusions closes the paper.

## 2. Numerical Simulation of Stochastic Dispersion

The starting point for our numerical studies is the efficient generation of independent realizations of random two-dimensional fields of log transmissivity, $Y(\mathbf{x}_i)$, viewed as a multivariate normal vector for any set of points $\mathbf{x}_i$. Usually, only the assumption of weak stationarity is made about $Y$ and the field is completely characterized by its expected value $\langle Y \rangle$ and covariance $C_Y(\mathbf{r})$, with $\mathbf{r}$ the planar distance vector between two points [e.g., *Dagan*, 1989].

Several numerical methods are available for this purpose, although not all of them are computationally efficient in view of the large domains required to track dispersing particles for sufficiently large travel distances in a convection field unaffected by boundaries.

*Clifton and Neuman* [1982] generated stationary, correlated fields with zero mean using a matrix method in which the number of computations is approximately proportional to the number $n$ of points in the computational grid and the storage is $O(n^2)$. Earlier a version of the nearest neighbor method had been applied by *Smith and Freeze* [1979] although the method neither guarantees stationarity of the generated fields nor a specified correlation structure. Inversion of an $n$ by $n$ banded matrix is required and storage is proportional to $n^2$. Methods based on fast Fourier transforms (FFT) have been developed [*Mantoglou and Wilson*, 1982; *Tompson et al.*, 1989; *Gutjahr*, 1989], considerably increasing the computational efficiency for large problems. The actual computations have employed the FFT-based method developed by *Gutjahr* [1989]. Preliminary numerical experiments [*Bellin*, 1991] indicated that at comparable sizes of the two-dimensional computational problem, Gutjahr's approach yields smaller spatial variations of the reconstructed covariance of $Y$ with respect to the turning band method [*Mantoglou and Wilson*, 1982; *Tompson et al.*, 1989]. Also, such a method proves more efficient computationally than matrix-based methods as the problem grows large.

In the present study, the log transmissivity covariance chosen is isotropic and exponential [*Gelhar and Axness*, 1983; *Dagan*, 1984; *Neuman et al.*, 1987; *Dagan*, 1989; *Sudicky*, 1986]:

$$C_Y(|\mathbf{r}|) = \sigma_Y^2 e^{-|\mathbf{r}|/l_Y} \tag{1}$$

where $\sigma_Y^2$ is the variance of the multivariate normal field $Y$ and $l_Y$ is the correlation scale of the field $Y$. In this study we do not consider nugget effects [*Dagan*, 1989, p. 359].

Figure 1 illustrates examples of reconstructed autocorrelations $\rho_Y = C_Y/\sigma_Y^2$ for a problem in which eight grid points per integral scale $l_Y$ are generated numerically in the range $0.05 \le \sigma_Y^2 \le 1.6$. Frequency cutoffs were set at $288 \times 288$ wave numbers in the example of Figure 1. The agreement of longitudinal correlations is excellent although transverse correlations slightly modify their integral scales. This effect, which has also been observed in applications of turning band codes unless a very large number of generation lines are employed (a procedure unsuitable to Monte Carlo iterations), is not shown by matrix-based methods (Figure 2) even for coarser grids. The example shown in Figure 2 used 32 generation lines for the turning band method with 2048 frequencies per line where the line discretization distance used was $l_Y/16$. The FFT method employed $288 \times 288$ wave numbers. The comparison is fair because we found experimentally that CPU time was equivalent in these conditions. The prohibitively large storage required by matrix methods in these conditions prevented their generalized use. The generation interval (up to $0.125\ l_Y$) has been adjusted in relation to convergence of computations (see section 4).

The Monte Carlo (MC) method is applied as follows:

1. For each successive iteration, independent realiza-

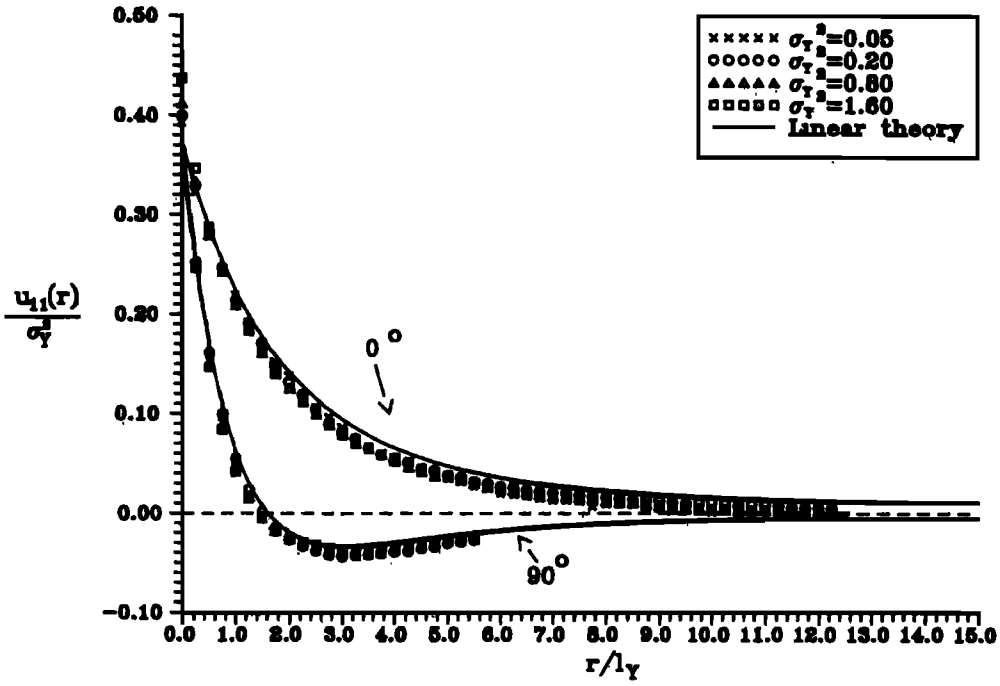


Fig. 4. Longitudinal velocity covariance function $u_{11}(r)$.

tions of the random field $Y$ are produced (characterized by the mean, the two-point covariance and the ratio $\eta$ of the correlation scale $l_Y$ to the grid size, the last feature having important computational consequences as discussed in what follows) in a rectangular domain of coordinates $(x_1, x_2)$ elongated in the direction of the mean flow $(x_1)$.

2. The mean head gradient $\mathbf{J} = (J, 0)$ and the porosity are assumed constant. The actual velocity field $\mathbf{V}(\mathbf{x})$ is obtained by solution of the following equations [e.g., *Dagan*, 1987]:

$$\nabla^2 h + \nabla h \cdot \nabla Y' = \mathbf{J} \cdot \nabla Y' \qquad \mathbf{V}(\mathbf{x}) = -\frac{T(x)}{n}(\nabla h - \mathbf{J}) \tag{2}$$

where $h(\mathbf{x})$ is the head fluctuation about the mean value $(-Jx_1)$; $Y' = Y(\mathbf{x}) - \langle Y \rangle$; $\mathbf{V} = \mathbf{U} + \mathbf{u}(\mathbf{x})$ is the Eulerian

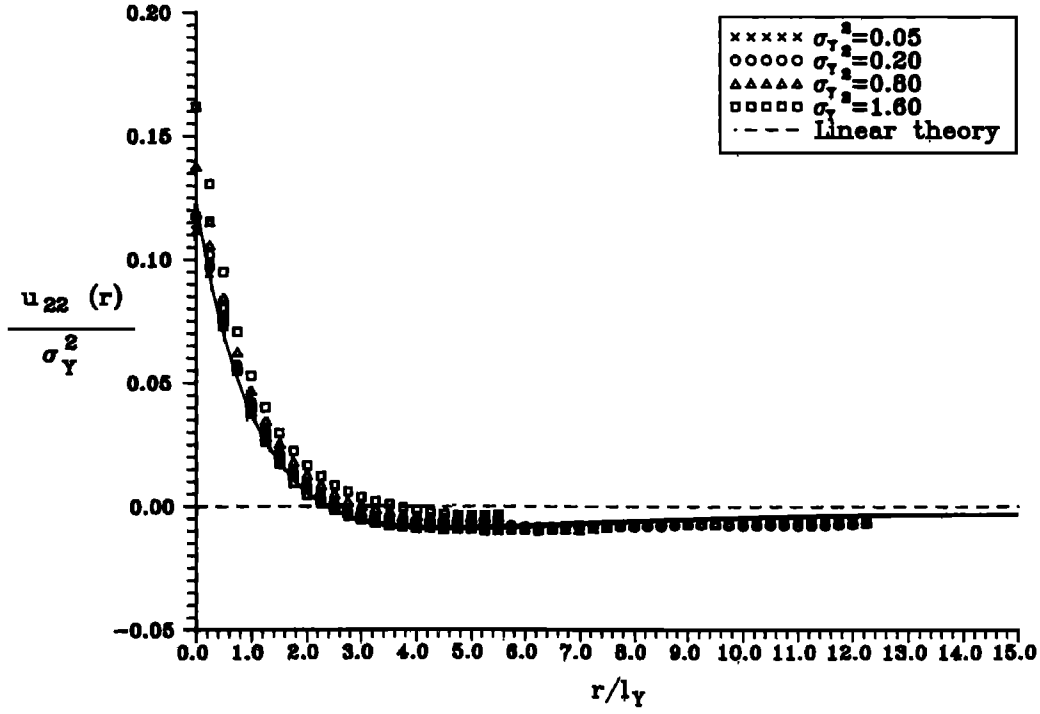


Fig. 5. Transverse velocity covariance function $u_{22}(r)$.

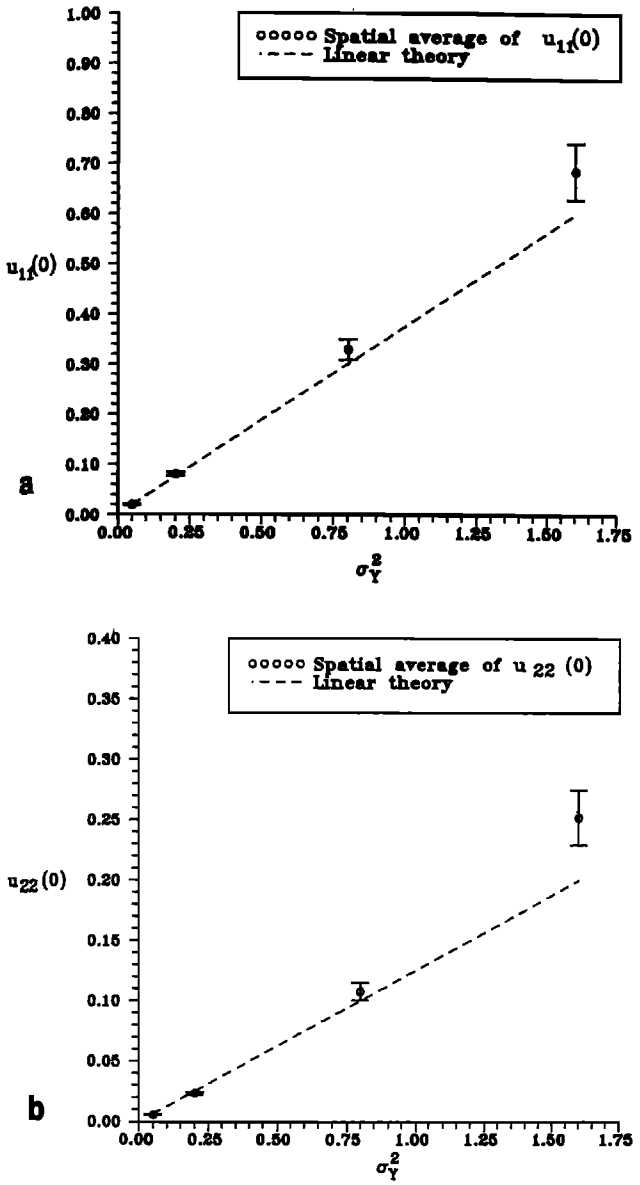


Fig. 6. Variance of computed (*a*) longitudinal and (*b*) transverse velocities as a function of $\sigma_Y^2$.

velocity; and $T = e^{Y(\mathbf{x})}$ is the lognormal transmissivity field [*Freeze*, 1975]. The mean velocity is therefore $\mathbf{U} = e^{\langle Y \rangle}\mathbf{J}/n$.

We refer to the solution of (2) as the solution of the flow equation. The approximation in (2), adopted by linear theories [*Dagan*, 1984; *Neuman et al.*, 1987; *Dagan*, 1989], and used in a $O(\sigma_Y^2)$ reformulation of the general problem, is:

$$\nabla^2 h = \mathbf{J} \cdot \nabla Y \qquad \mathbf{V}(\mathbf{x}) = -\frac{e^{\langle Y \rangle}}{n}(\nabla h - \mathbf{J}(1 + Y')) \qquad (3)$$

Computations are performed in dimensionless form with reference to the scales $l_Y$, $Jl_Y$, $l_Y n/\langle T \rangle J$, and $\langle T \rangle \mathbf{J}/n$ for length, head, time and velocity respectively, where $\langle T \rangle = \exp[\langle Y \rangle + (1/2)\sigma_Y^2]$.

The actual velocity field $\mathbf{V}(\mathbf{x})$ is obtained from a suitable finite element solution of the boundary value problem defined by (2) and deterministic boundary conditions of the first type [e.g., *Pinder and Gray*, 1977; *Gambolati*, 1980; *Johnson*, 1987]. The solver employed for the resulting algebraic system was the conjugate gradient method (GCM) with incomplete Cholesky acceleration [*Gambolati*, 1988]. The flow domain is rectangular, $36l_Y$ by $18l_Y$ wide. The major length is in the direction $x_1$ of mean flow. The discrete transmissivity field is generated in 288 by 144 square blocks of size $l_Y/8$. The finite element grid is obtained by subdividing each integral scale into up to 32 triangular elements according to convergence of computations (see also section 5). Linear shape functions allow for velocities constant within an element. Convergence of computations (see section 4) assures the reliability of the computational results under these conditions (G. Gambolati, personal communication, 1992). The total number of elements is 20,736 and that of the nodes is 10,585. The deterministic boundary conditions imposed are no flux at $x_2 = 0$ and $x_2 = 18l_Y$ and unit specific discharge in the $x_1$ direction at the nodes of coordinates $(0, x_2)$ and $(36l_y, x_2)$. The condition $h = 0$ is imposed for the node $\mathbf{x} = (0, 0)$.

It is interesting to observe that the deterministic boundary conditions affect considerably the domain suited for solving the transport equation [*Rubin and Dagan*, 1988, 1989]. Computed velocity variances $\sigma_u^2$ are plotted (Figures 3*a* and 3*b*) to define an inner core region unaffected by boundaries. Only in the region where the variance is constant can particles be tracked without bias. It is clear from the computations that at increasing values of $\sigma_Y^2$ the test area is significantly reduced, even exceeding the indications of a biased belt of $3I_Y$. Such an indication is drawn, somewhat arbitrarily, from theoretical results [*Rubin and Dagan*, 1989] on the head variogram in a flow field where the boundary conditions are of constant head. Although it is not entirely clear whether the influence of boundaries is a numerical effect or is due to genuine nonstationarity as in the work by *Rubin and Dagan* [1989], at $\sigma_Y^2 = 2$ a meaningful portion of the velocity field is affected by boundary conditions and the corresponding results would be inconclusive. For this reason we restricted our attention to the cases where $\sigma_Y^2 \leq 1.6$.

It is to be observed that the final aim of the flow analysis is the computation of the statistics of velocity, e.g., the covariance function $u_{jl}(\mathbf{r}) = \langle u_j(0)u_l(\mathbf{r}) \rangle$ where $u_j$ is the velocity fluctuation about the mean $U_j$ along the $x_j$ direction, which is used in transport theory. A general first-order approximation for the analytical velocity covariance is available [*Neuman et al.*, 1987; *Dagan*, 1984] as a function of the velocity and log conductivity covariance spectra. Comparison with the explicit solution for $u_{jl}$ obtained assuming the covariance structure (1) in the two-dimensional case [*Rubin*, 1990] will yield an estimate of nonlinear effects in the solution of the flow equation.

3. The transport theory deals with the determination of the spatial moments of the concentration distribution which, in the case of passive solute studied in this context, are computed by the moments of the displacement distribution of dispersing particles [*Taylor*, 1921]. Ensemble averaging is made upon releasing only one particle for each random transmissivity field so as to generate only uncorrelated paths (pore scale dispersion is neglected in this study, i.e., $Pe = \infty$ where $Pe$ is the proper Peclet number). The trajectory $\mathbf{X}_r(t; \mathbf{x}_0, t_0)$ of the particle starting at time $t_0 = 0$ from an inner initial position $\mathbf{x}_0 = (5l_Y, 9l_Y)$ can be computed by

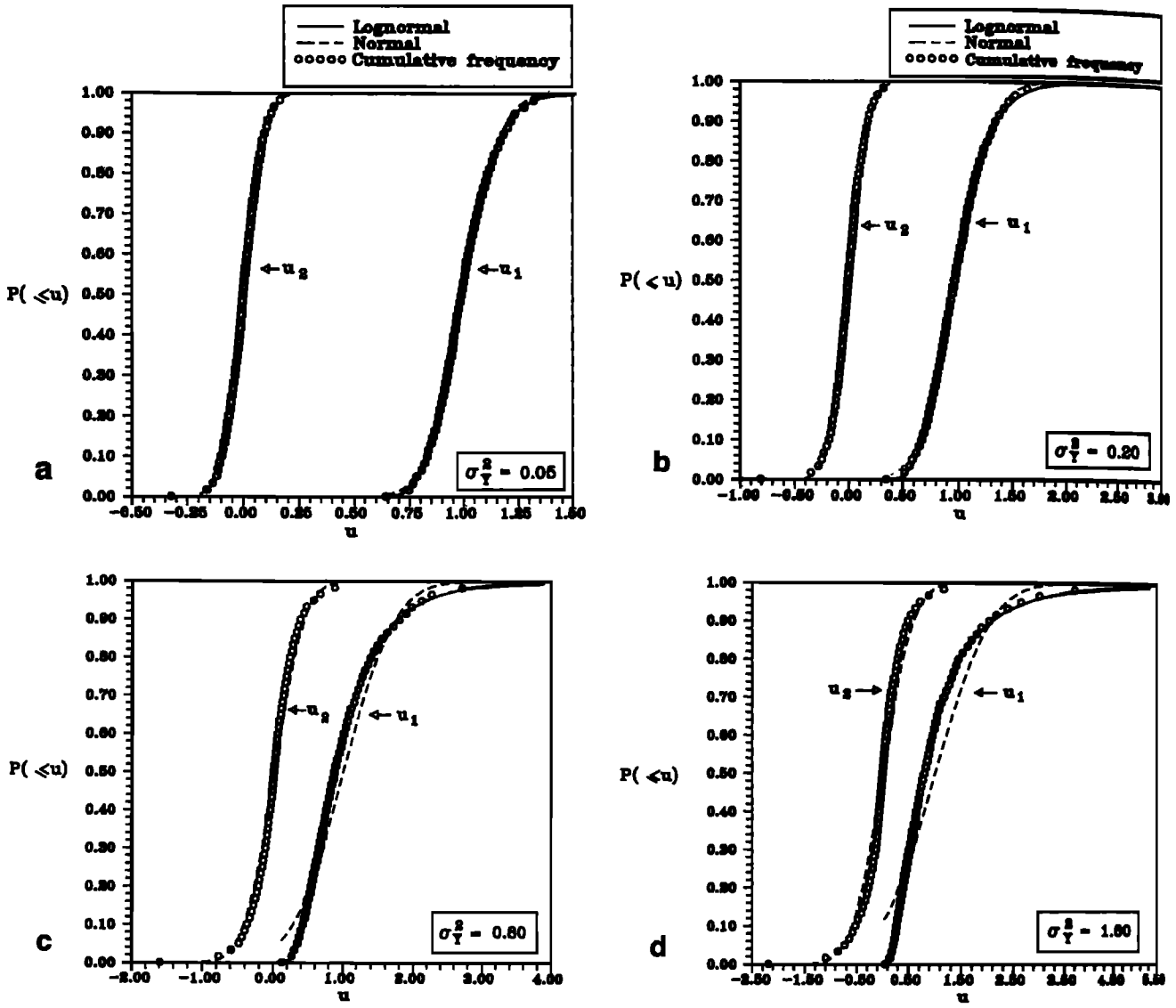


Fig. 7. Cumulative frequencies of computed longitudinal and transverse velocities for (*a*) $\sigma_Y^2 = 0.05$, (*b*) $\sigma_Y^2 = 0.2$, (*c*) $\sigma_Y^2 = 0.8$, and (*d*) $\sigma_Y^2 = 1.6$.

$$\mathbf{X}_t(t;\ \mathbf{x}_0,\ 0) = \mathbf{x}_0 + \mathbf{U}t + \int_0^t \mathbf{u}(\mathbf{X}_t(\tau;\ \mathbf{x}_0,\ 0))\ d\tau$$

$$= \mathbf{x}_0 + \mathbf{U}t + \mathbf{X}' \qquad (4)$$

*Dagan* [1984, 1987] proposed a linear theory in which the basic equation for the second moments $X_{jl}(t) = \langle X_j'(0)X_l'(t)\rangle$ of particle displacements as a function of the velocity covariance function [*Dagan*, 1984],

$$X_{jl}(t) = 2\int_0^t (t-\tau)u_{jl}(U\tau)\ d\tau \qquad (5)$$

allows closed-form solutions in the case of the exponential covariance for $Y$ considered in this paper. Pore scale dispersion is neglected in (5) and in the present computations. These solutions will be compared with all numerical solutions.

The trajectory of the particle, computed by discretizing (4), i.e., a particle-tracking procedure, is recorded at discrete time intervals. The discrete time step is computed from local velocities to avoid particles' bypassing one or more elements in a single time step. This procedure ensures also that even for the largest $\sigma_Y^2$ tested the particles provide a sample of all computed velocities.

The particle trajectory (4), of components $X_1$ and $X_2$ in the longitudinal and transverse directions, is computed numerically with reference to a time interval $\Delta t$ and at the $i$th MC iteration by a discrete first-order scheme [e.g., *Øksendal*, 1988], where $N\Delta t$ is the maximum travel time (corresponding to travel distances exceeding the inner core region of unbiased velocities). The statistical moments of particles' trajectories are computed with reference to averages over $M$ Monte Carlo iterations.

The steps 1 through 3 are repeated until the statistics of ensemble averaging of the transport variables (mean trajectory, longitudinal and transverse second moments) show negligible variations with increasing number of iterations. Most computations (see section 5) required up to 1500 MC iterations to stabilize second-order moments.

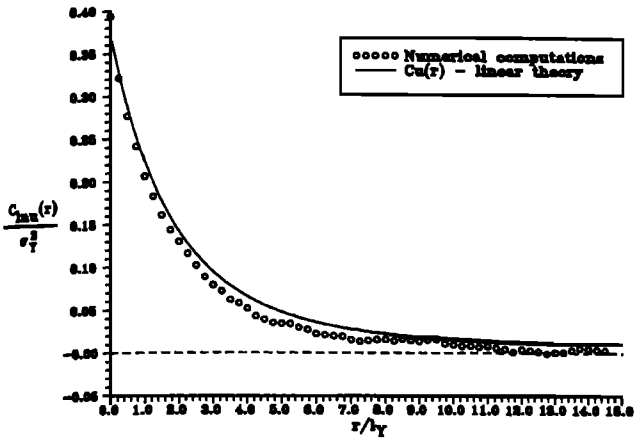


Fig. 8. Covariance function of the logarithm of longitudinal velocity.

## 3. STATISTICS

Figures 4 and 5 illustrate the results of the computation of dimensionless covariance functions $u_{11}(r)$, $u_{22}(r)$ for longitudinal and transverse velocities. The numerical results, obtained by averaging over the central core ($8I_Y$ by $8I_Y$ wide) unaffected by boundary conditions, are compared with the linear solution [*Rubin*, 1990]. From the results we argue that, at second order, significant differences in the correlation structure are shown only within a limited radius of influence in the proximity of the origin of the spatial lag (where, according to the linear theory, $u_{11}(0) = 3/8\sigma_Y^2$, $u_{22}(0) = 1/8\sigma_Y^2$).

Figures 6*a* and 6*b* show another interesting result concerning the statistics of velocity. The variances $u_{11}(0)$ and $u_{22}(0)$ are computed (within the inner core region) by ensemble averaging over 1500 realizations in all different spatial locations (mesh points) inside the inner core region. The ensemble average hence varies from point to point, allowing the estimation of its spatial mean and standard deviation. In Figures 6*a* and 6*b* the spatial mean values of $u_{11}(0)$ and $u_{22}(0)$ are plotted with their interval of confidence (estimated by three standard deviations) as a function of the log conductivity variance of $\sigma_Y^2$. We observe a consistent increase of the confidence interval with increasing heterogeneity as expected, and a progressive departure from the linear relation with 3/8 and 1/8 slope.

Figures 7*a*–7*d* show computed (cumulative) probability distributions for longitudinal and transverse velocities at $\sigma_Y^2 = 0.05, 0.2, 0.8, 1.6$ based on ensemble averaging with 1500 realizations. Maximum likelihood fits for normal and lognormal distributions are also shown. From the graphs one clearly infers the tendency of longitudinal velocities to be represented by a skewed distribution. The departure from the (linear) Gaussian shape is already observed at $\sigma_Y^2 \geq 0.2$. This tendency is not shown by transverse velocities, which remain normal even at the highest degrees of heterogeneity tested here.

To investigate this peculiarity further, Figure 8 shows a comparison of the covariance $C_{\ln u}(\mathbf{r})$ of the logarithm of longitudinal velocity and the unmodified linear solution for the case $\sigma_Y^2 = 0.20$. It is interesting to observe that if velocities and their logarithms have similar correlation structures their distribution may approximate lognormality. In this case, in fact, on expanding an (arbitrary) covariance $C_u(\mathbf{r})$ of velocities (assumed lognormally distributed) in Taylor series the following relation is obtained:

$$C_{\ln u}(\mathbf{r}) = \frac{C_u(\mathbf{r})}{U^2} + O(\sigma_Y^4) \tag{6}$$

which may serve as an indicator. Nevertheless, from the results we argue that differences are larger than $O(\sigma_Y^4)$.

Figure 9 shows the results of the computation of third-order moments for longitudinal velocities as a function of $\sigma_Y^2$. The interval of confidence here is one standard deviation, computed from the spatial variations in the inner core region. The geometric departure from the null third moments of the normal distribution clearly supports our conjecture on the noteworthy role of nonlinear terms. Similarly, Figure 10

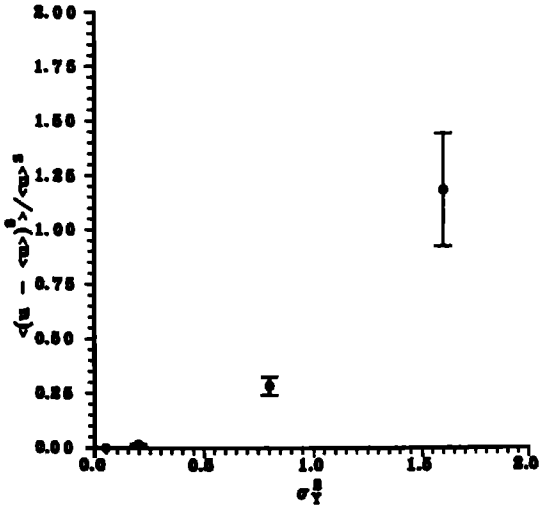

Fig. 9. Third moments of computed longitudinal velocities as a function of $\sigma_Y^2$.

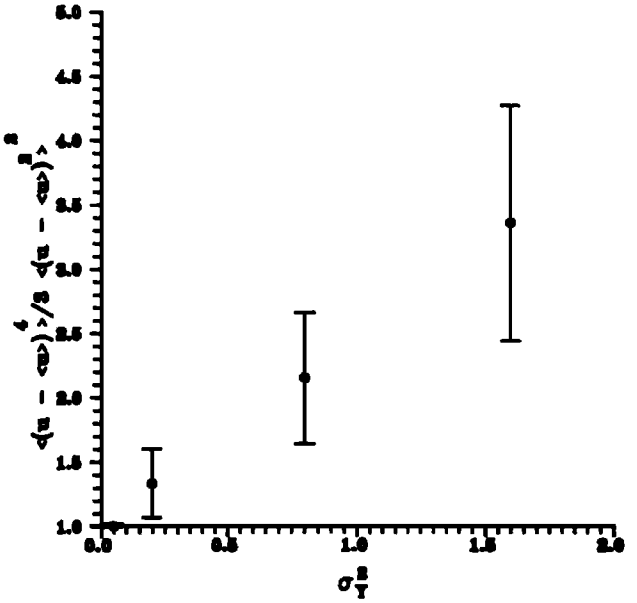

Fig. 10. Fourth-order moments (normalized by the corresponding values of the Gaussian distribution) of computed longitudinal velocities as a function of $\sigma_Y^2$.

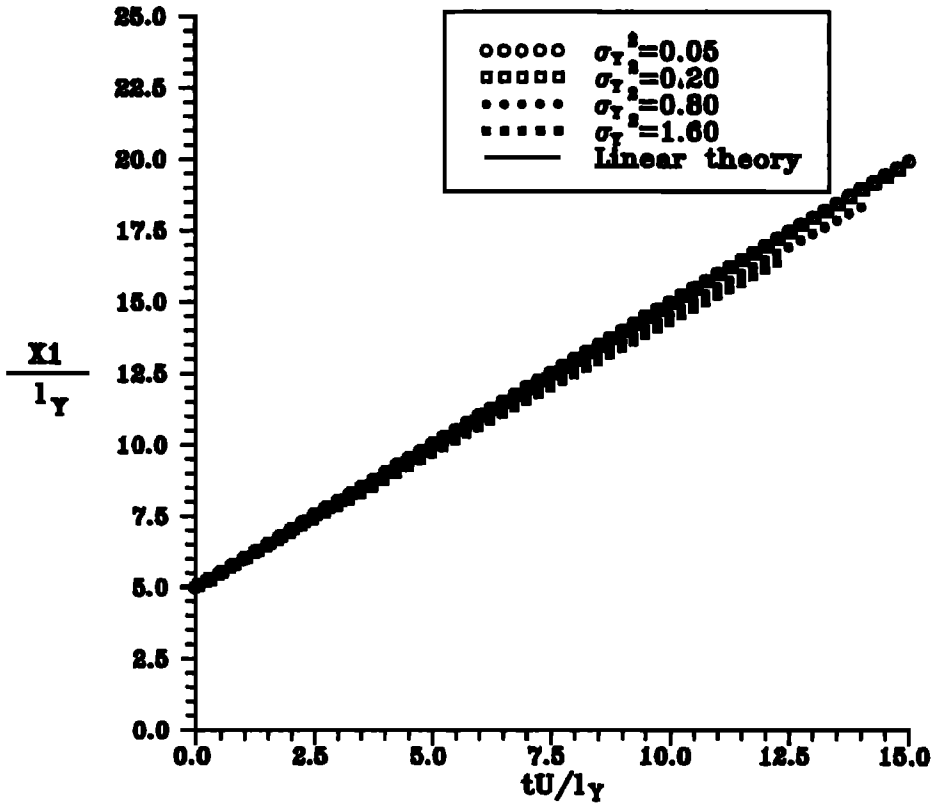


Fig. 11. Lagrangian mean trajectories.

shows fourth-order moments normalized by the values of the Gaussian distribution. The interval of confidence is defined by one standard deviation. The departure from the normal distribution is therefore statistically significant, in any case, as $\sigma_Y^2 > 0.2$.

Assessing lognormality proves more difficult. In fact, if $u$ is indeed lognormal, simple relationships between the moments of $u$ and ln ($u$) can be established (i.e., $\langle u \rangle = \exp(\langle \ln u \rangle + \sigma^2_{\ln u}/2)$, and $\langle (u - \langle u \rangle)^n \rangle = f_n(\sigma^2_{\ln u})$ where $f_n$ are known functions (G. Dagan, personal communication, 1991). If we use such relationships for, say, $\sigma_Y^2 = 1.6$ and assume $\sigma^2_{\ln u} = (3/8)\sigma_Y^2 = 0.60$, then $\langle (u - \langle u \rangle)^3 \rangle / \langle u \rangle^3 = 2.6$, i.e., roughly twice the result of Figure 9. Similarly, $\langle (u - \langle u \rangle)^4 \rangle / 3\langle (u - \langle u \rangle)^2 \rangle^2 = 10$, about 3 times the result of Figure 10. Also the second moment $\langle (u - \langle u \rangle^2 \rangle / \langle u \rangle^2$ is larger than the value in Figure 6. These discrepancies suggest that $u$ is somewhere between normality and lognormality. As a likely consequence only complex theoretical closures similar to those of the problem of turbulence [e.g., *Lundgren and Pointin*, 1975; *Kraichnan*, 1970] might be thought of as appropriate.

We also observe (Figure 11) that at increasing heterogeneity the mean Lagrangian trajectory slightly deviates from the Eulerian value of ($Ut$, 0). This effect is perceived for $\sigma_Y^2 \geq 0.8$. Since theoretically Eulerian and Lagrangian mean velocities are equal (a result known from the turbulence literature (G. Dagan, personal communication, 1991)), an explanation of this Lagrangian retardation rests on numerical accuracy alone.

## 4. Convergence of Computations

Accuracy of computations is crucial to establish the validity of the theoretical points addressed. Here we need to establish two types of convergence: (1) that of the numerical solution; and (2) that of statistical quantities obtained by ensemble averaging over Monte Carlo iterations.

With reference to the second type, one first observes that substantially different rates of convergence hold for different statistical moments [*Salandin et al.*, 1991]. While the experimentally determined mean trajectories (via ensemble averaging) approach the asymptotic values and the theoretical predictions with few iterations regardless of the model employed (fully nonlinear, partially linearized), at increasing values of $\sigma_Y^2$ the number of iterations required to stabilize second-order moments also increases. To quantify this effect, Figures 12*a* and 12*b* show results of simulations of fully nonlinear flow (i.e., the solution to (2)) and transport and, for the sake of comparison, of the solution characterized by linear flow (i.e., the solution to (3)) and nonlinear transport, which is commonly adopted by theoretical [e.g., *Neuman and Zhang*, 1990] or numerical [e.g., *Rubin*, 1990] studies. The results shown are the longitudinal (Figure 12*a*) and transverse (Figure 12*b*) displacement variances $X_{11}/l_Y^2$ and $X_{22}/l_Y^2$ averaged progressively over 100, 500, 1000 and 1500 MC realizations at $\sigma_Y^2 = 0.2$. Analogous results are presented in Figures 13 and 14, respectively, for $\sigma_Y^2 = 0.8$ and 1.6. It is to be observed that simulations are stopped at arbitrary travel times (e.g., Figures 13, 14), whenever a

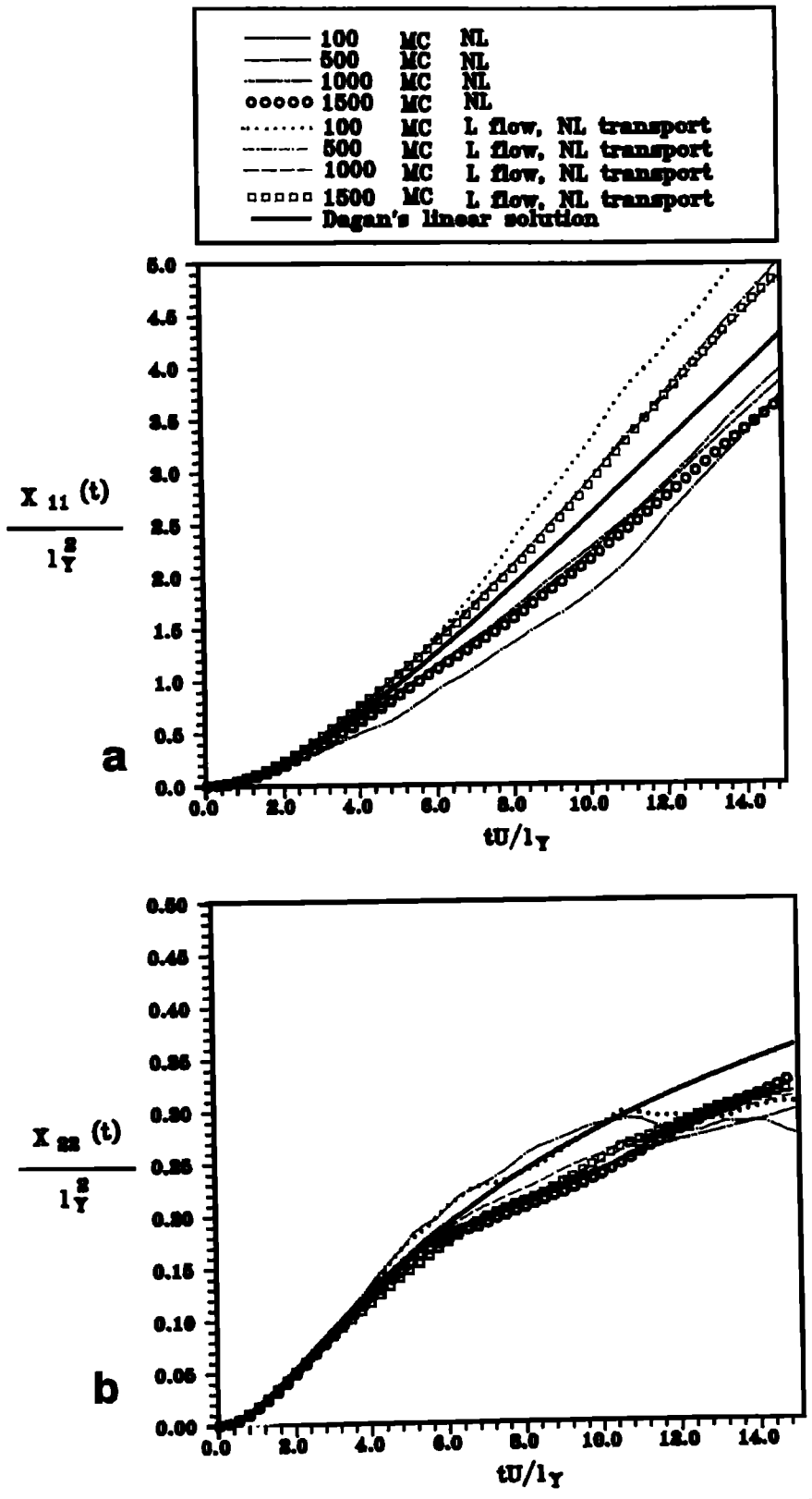


Fig. 12. (*a*) Longitudinal and (*b*) transverse displacement variances as a function of dimensionless time averaged over increasing MC runs ($\sigma_Y^2 = 0.2$).

single particle transits the inner core region. The probability of such an occurrence grows with increasing values of $\sigma_Y^2$.

We observe that stabilization of second moments occurs after hundreds of iterations even for relatively small values of $\sigma_Y^2$, in particular for the transverse variance. This is an interesting result. In fact, on one hand it suggests as a general methodology in MC-type studies to adjust the number of iterations to the convergence of the highest moment of

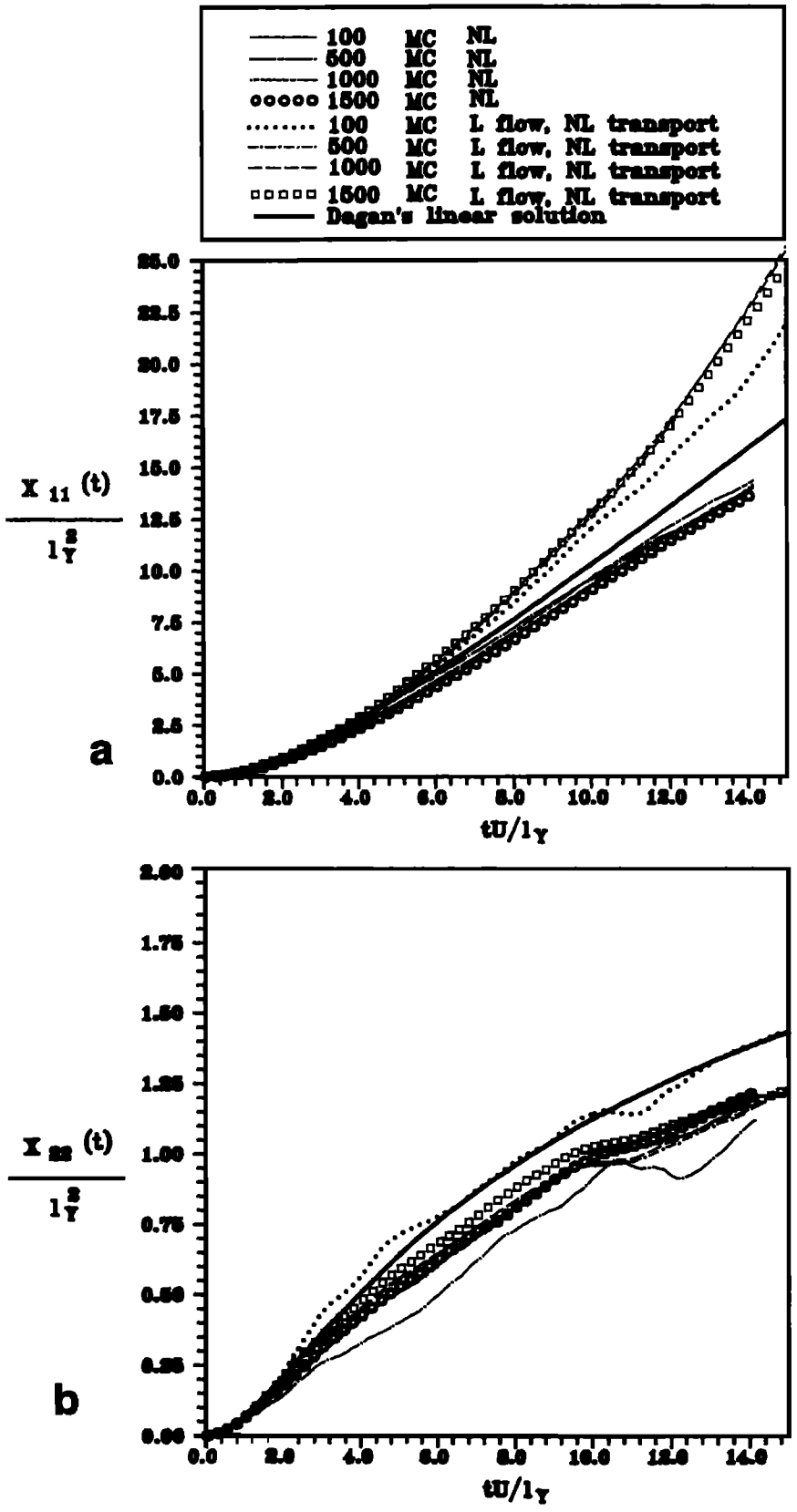


Fig. 13. (*a*) Longitudinal and (*b*) transverse displacement variances as a function of dimensionless time averaged over increasing MC runs ($\sigma_Y^2 = 0.8$).

interest; on the other hand, the results in Figures 12–14 have implications for the spatial extent of single-realization studies of stochastic dispersion. Such studies, in fact, [e.g., *Tompson and Gelhar*, 1990; *Ababou et al.*, 1989] postulate that spatial averaging over a sufficiently large domain (say, sampling enough independent trajectories) might mimic ensemble averaging. A measure of the number of independent trajectories is the extent of the domain transverse to the

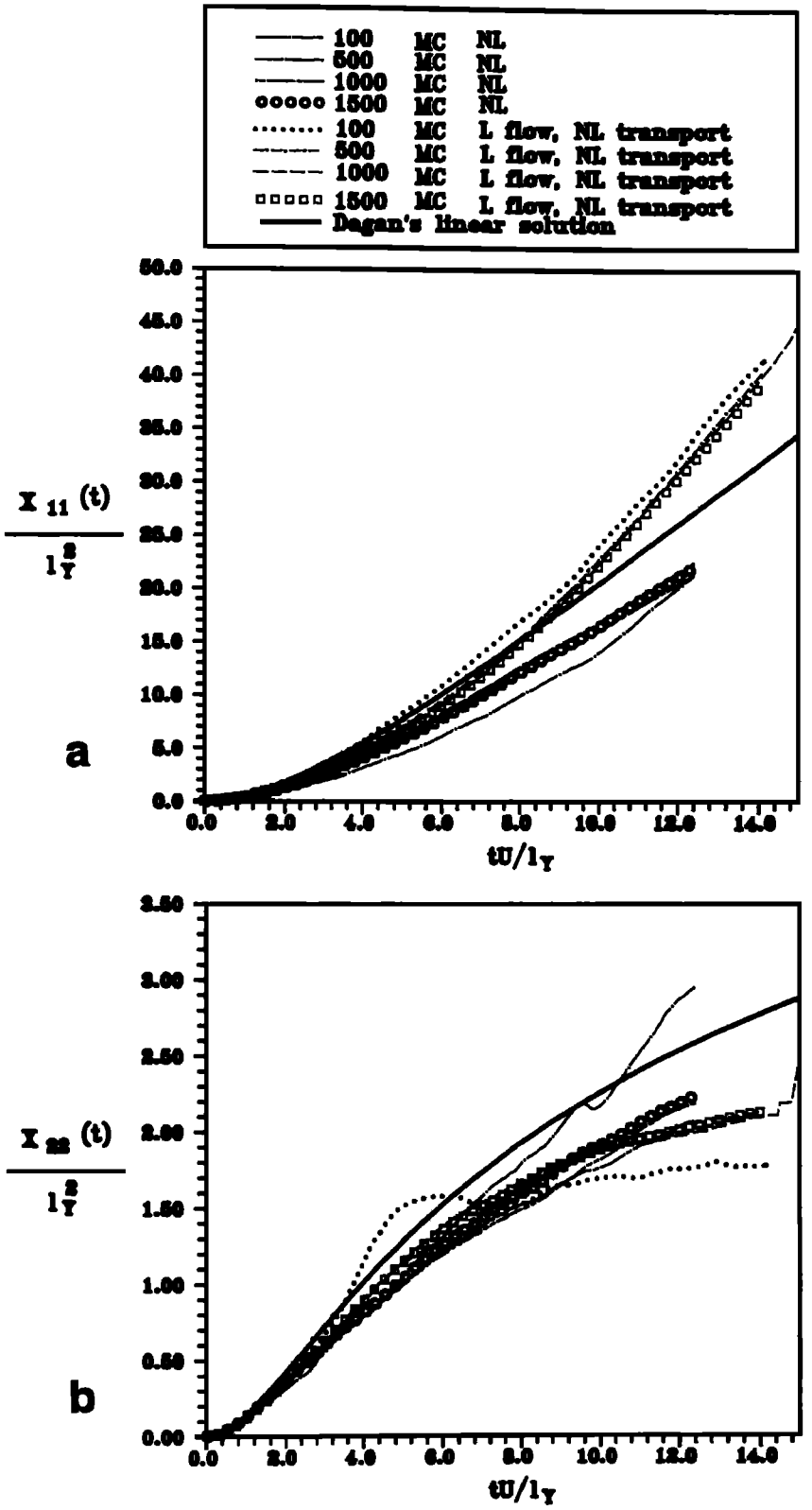


Fig. 14. (*a*) Longitudinal and (*b*) transverse displacement variances as a function of dimensionless time averaged over increasing MC runs ($\sigma_Y^2 = 1.6$).

mean flow measured by the number of integral scales spanning the possible initial positions of the dispersing particles. This measures the quantity of independent information on which to build the statistics. Our results would therefore suggest the need for quite large dimensions of one-realization studies as the variance of log conductivity grows large.

The first of the two types of convergence required to assess the validity of the present results (alluded to at the beginning of this section) deals with the size of the compu-

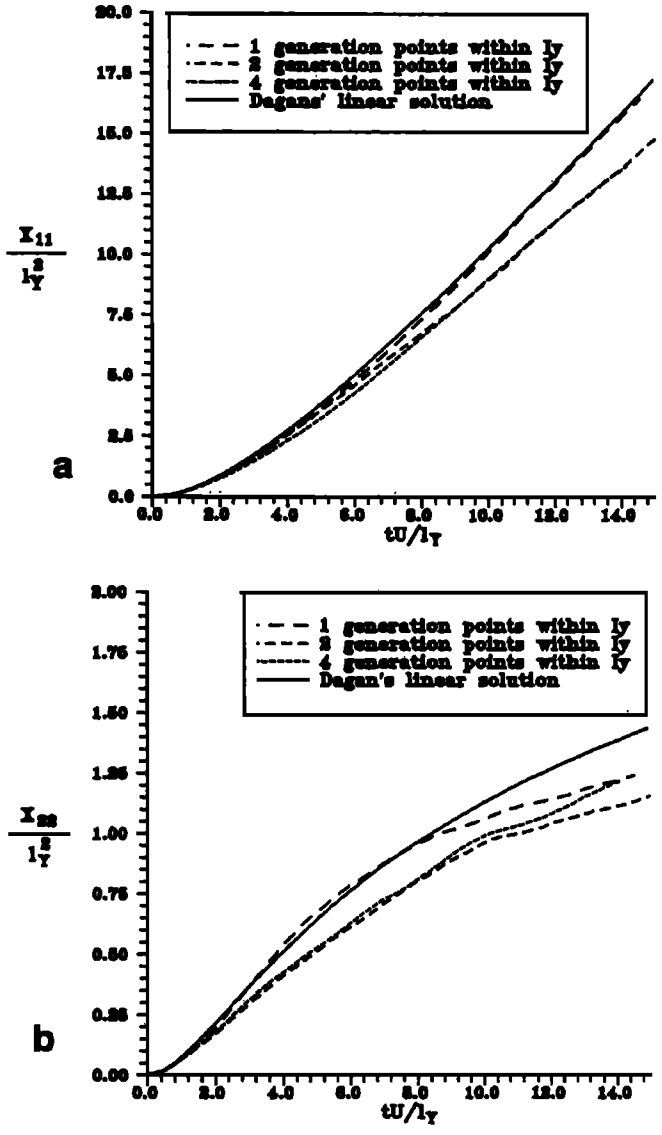


Fig. 15. (*a*) Longitudinal and (*b*) transverse computed displacement variances as a function of dimensionless time for different sizes $\eta$ of the generation mesh ($\sigma_Y^2 = 0.8$).

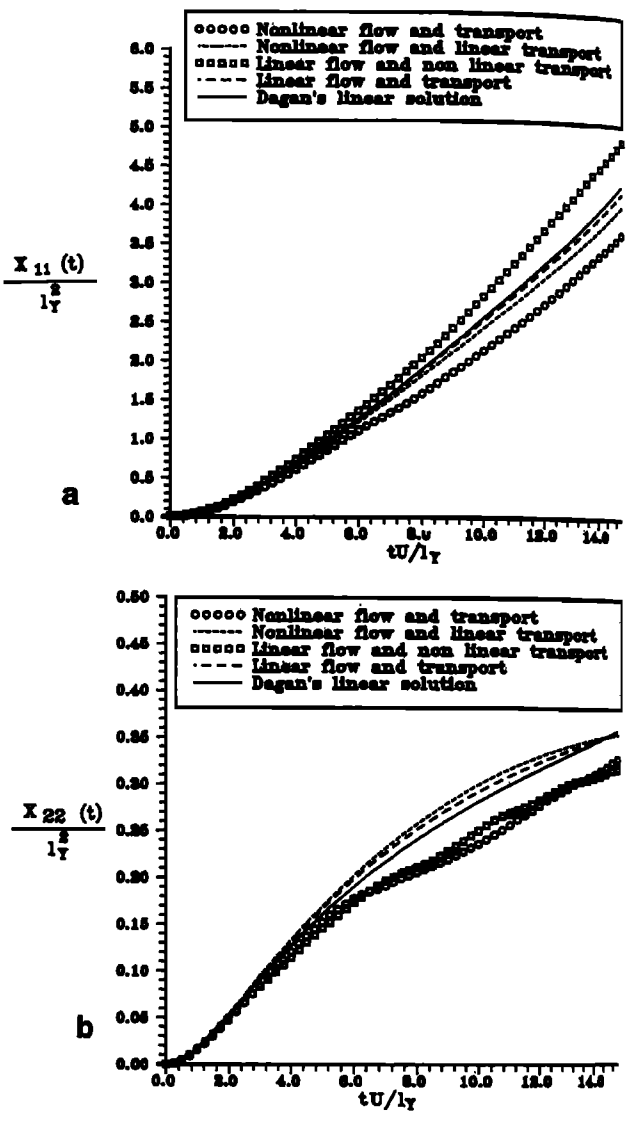


Fig. 16. (*a*) Longitudinal and (*b*) transverse displacement variances as a function of dimensionless time computed by five different mathematical models ($\sigma_Y^2 = 0.2$).

tational mesh compared with the scale of heterogeneity (i.e., the integral scale $I_Y$), i.e., the number of generated mesh points per integral scale required to reach convergence of second-order moments of displacements. *Ababou et al.* [1989] suggested that discretization effects may be avoided when the ratio $\eta$ of discretization scale to integral scale is $\eta \geq 1 + \sigma_Y^2$. *Valocchi* [1990] chose, for safety, to employ as many as 10 generated points per integral scale, although in single-realization studies.

Here we chose to test convergence experimentally for second-order moments. As an example, Figures 15*a* and 15*b* show the longitudinal and transverse displacement variance ($\sigma_Y^2 = 0.8$) computed for ratios $\eta = 1$, 2 and 4, the latter two obeying Ababou's criterion. All fields were regenerated at increasing resolutions, and a posteriori checking assured that no variance reduction was artificially created. Longitudinal displacement variances show clear convergence, no significant difference being observed in the transition from $\eta = 2$ to $\eta = 4$. Convergence is less pronounced for transverse variances. Interestingly, the computations for a ratio $\eta = 1$ show an artificially good agreement with the linear solution due to an artificial increase in the actual integral scale $I_Y$ as a result of discrete approximations. Also, a coarse discretization of the heterogeneous $Y$ field induces an artificial linearization of the numerical flow field because of filtering of high frequencies.

In a similar manner the ratio $\eta = 4$ proved appropriate for the most heterogeneous field investigated herein ($\sigma_Y^2 = 1.6$).

## 5. First-Order Theories

Figures 16*a* and 16*b* show longitudinal and transverse (dimensionless) displacement variances computed for $\sigma_Y^2 = 0.2$ by five models: (1) *Dagan*'s [1984] analytical solution; (2) the fully nonlinear numerical solution (defined by the mathematical model of (2), and a convergent and accurate numerical model); (3) a fully linear numerical solution obtained solving (3) and (5); (4) a partially nonlinear solution of the

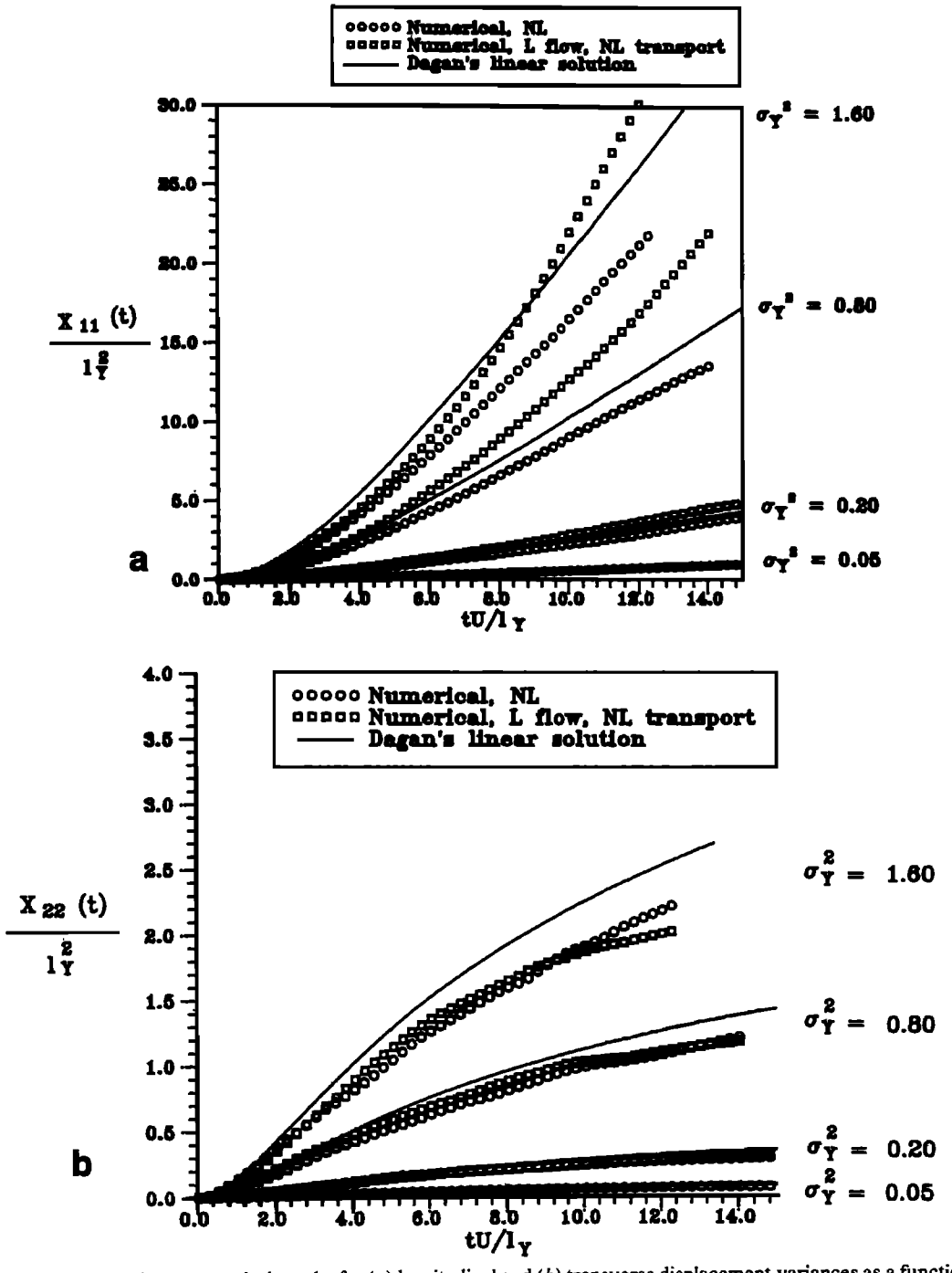


Fig. 17. Fully nonlinear numerical results for (*a*) longitudinal and (*b*) transverse displacement variances as a function of dimensionless time ($\sigma_Y^2 = 0.05, 0.2, 0.8, 1.6$).

first type, characterized by a linearized flow evaluation (equation (3)) and nonlinear transport computations (by particle tracking; see section 3); and (5) a partially nonlinear solution of the second type, characterized by nonlinear flow (computed as in the second model) and linear transport computations. The latter is simply computed, e.g., for the longitudinal displacement variance $X_{11}$, by:

$$X_{11}(t) = 2\int_0^t d\tau(t-\tau)u_{11}(U_L\tau) \qquad (7)$$

where a numerical estimate of Lagrangian mean velocity $U_L$ and of the nonlinear velocity covariance $u_{11}$ are employed.

The numerical solution of the linearized equations matches well the analytical results, hence proving the soundness of the procedures. The fully nonlinear model yields smaller variances, both longitudinal and transverse. The foremost result in Figure 16 is that nonlinear contributions to the longitudinal displacement variance yield counteracting (and nonadditive) contributions to the dispersion process. It is suggested, therefore, that part of the unexpectedly broad

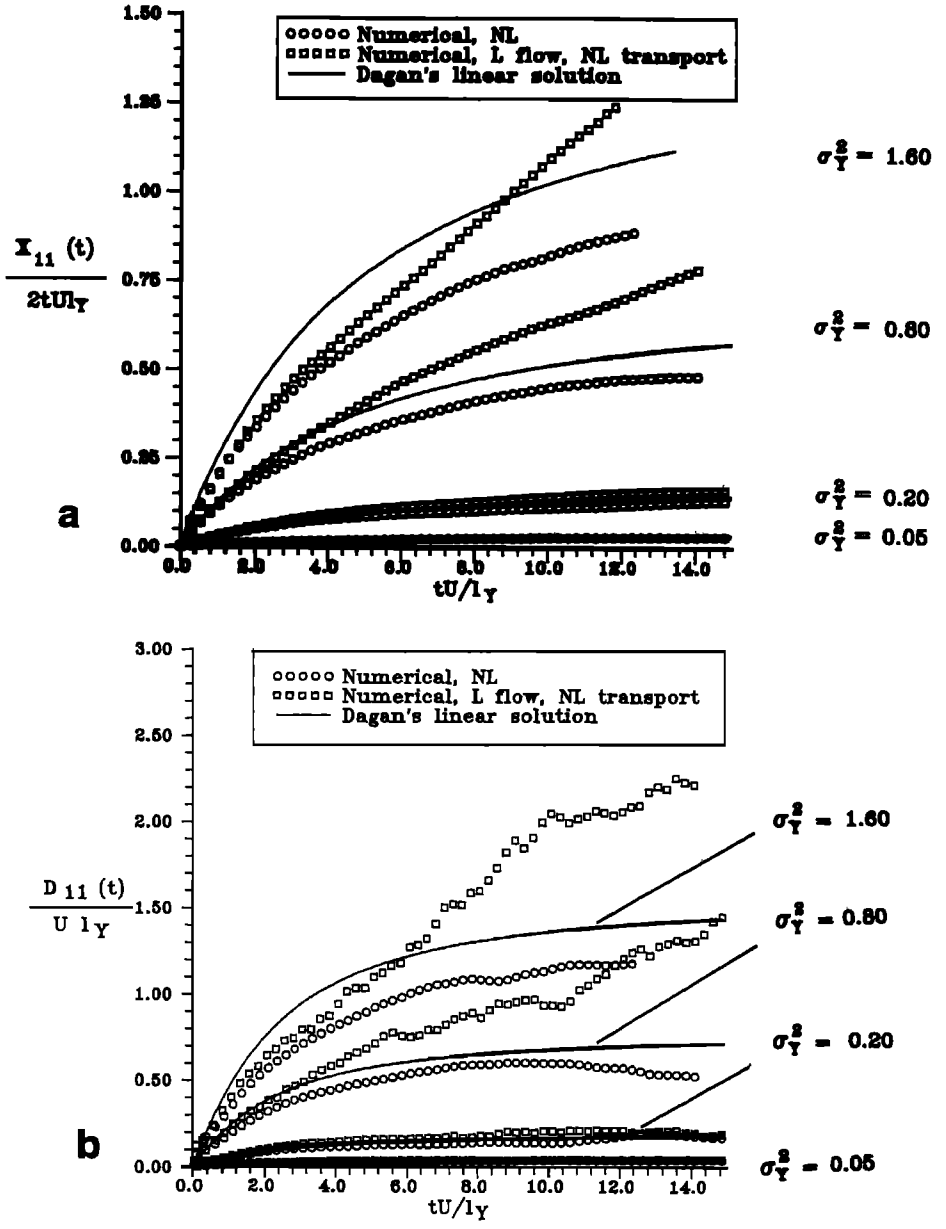


Fig. 18. (*a*) Apparent longitudinal dispersion coefficient as a function of dimensionless time ($\sigma_Y^2 = 0.05, 0.2, 0.8, 1.6$). (*b*) Dispersion coefficients estimated by numerical differentiation.

range of validity of the linear solution (see Figure 17) might be due to the difference in sign of the errors induced by the linearizations of flow and transport. Transverse displacements are, as usual, harder to judge, although, in general, opposite signs of linearization errors are also evidenced.

It is also interesting (Figures 17*a* and 17*b*) that, as suggested previously [*Salandin and Rinaldo*, 1990], reformulation of the same problem with a linearization of the flow equation alone, an assumption often accepted in theoretical and numerical studies on this subject, yields deviations from linear theory larger than those induced by a fully nonlinear solution. Some doubts are therefore cast on previous conclusions drawn on the limitations of the linear theory based on partially linearized equations [e.g., *Rubin*, 1990]. This is more evident (Figure 18) in terms of dispersion coefficients. Besides taking a numerical derivative of the computed variances (i.e., $D_{11} = 1/2dX_{11}/dt$) (Figure 18*b*)), Figure 18*a* illustrates, for the sample case of the longitudinal dispersion coefficient, the apparent (dimensionless) dispersion coefficient ($D_{11} = X_{11}/(2tUI_Y)$). The macroscopic effect of the linearization in the flow equation alone seems to yield an overestimation of the longitudinal dispersivity and an underestimation of the transverse dispersion. The latter result is not confirmed by other numerical findings [e.g., *Rubin*, 1990].

Travel time statistics are important [*Dagan and Nguyen*, 1989; *Shapiro and Cvetkovic*, 1988; *Dagan*, 1989] because they are robust in characterizing the dispersion process, blending all sources of uncertainty into a unique curve. Figures 19*a*–19*d* illustrate travel time distributions at three distinct absorbing barriers (placed normal to the mean flow, respectively, at distances $L/I_Y$ 2.5, 7.5 and 17.5) computed

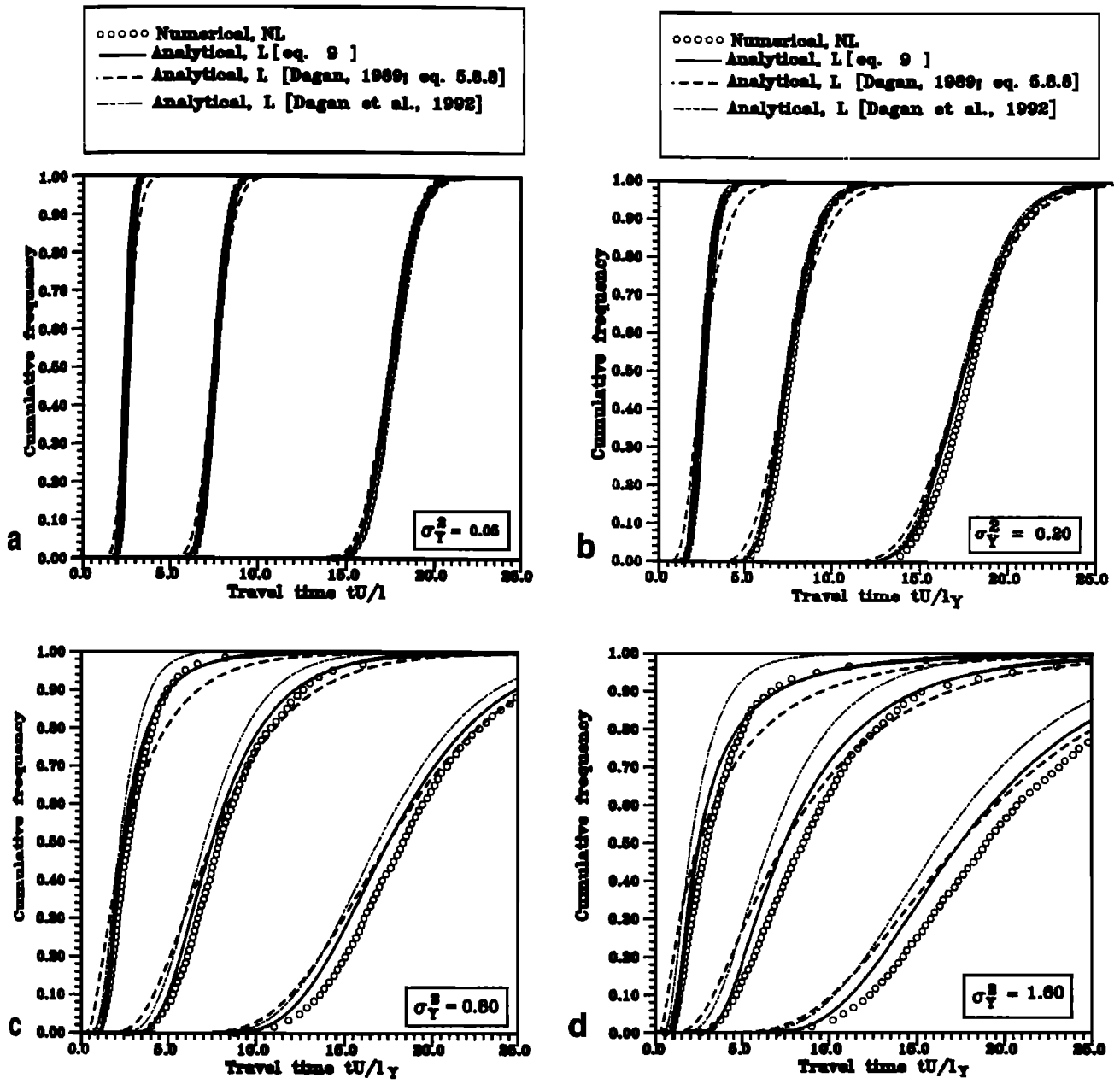


Fig. 19. Travel time distributions at $(x_1 - x_0)/I_Y = 2.5, 7.5, 12.5$: (*a*) $\sigma_Y^2 = 0.05$; (b) $\sigma_Y^2 = 0.2$; (c) $\sigma_Y^2 = 0.8$; and (*d*) $\sigma_Y^2 = 1.6$.

by the fully nonlinear model and two analytical models. The figures are relative to the statistics of the experiments with $\sigma_Y^2 = 0.05$ to 1.6.

The first analytical model is that of *Dagan and Nguyen* [1989] in which the longitudinal dispersion coefficient is constant (say, $D_{11}(\infty)$), transverse dispersion in this case does not play any role [*Dagan*, 1989], yielding a travel time probability $G(t, L)$ of a particle, injected at x = 0 at time $t = 0$ to reach a distance $L$ in the longitudinal direction, given by

$$G(t, L) = \frac{1}{2}\left[1 - \text{erf}\left(\frac{L - Ut}{[4D_{11}(\infty)t]^{1/2}}\right)\right] \tag{8}$$

(where erf denotes the error function) with usual notation. Equation (8) is supposed to apply asymptotically for large $Ut/I_y$ when $D_{11}(t) \to D_{11}(\infty)$. Although to use (8) does not seem warranted, in particular for the control plane close to the source, we observe its robustness in all cases tested herein. This has theoretical implications, e.g., for the interpretation of field tests, because Dagan's theory predicts that $D_{11}(\infty) = \sigma_Y^2 I_Y U$ regardless of the detailed covariance structure of the transmissivity field. The second analytical model allows time-dependent dispersion coefficients [*Bellin*, 1990; *Rinaldo et al.*, 1991] to yield

$$G(t, L) = \frac{1}{2}\left[1 - \text{erf}\left(\frac{L - Ut}{[2X_{11}(t)]^{1/2}}\right)\right] \tag{9}$$

where $D_{11}(t) = 1/2dX_{11}/dt$. The time evolution of $X_{11}(t)$ is given by the theoretical values of *Dagan*'s [1984] linear solution. We observe a better performance of (9), as ex-

pected, for small travel distances and relatively large heterogeneity. *Shapiro and Cvetkovic*'s [1988] theoretical travel time distributions are also plotted upon substitution of the harmonic mean velocity, as in the original formulation, by the arithmetic mean. In fact, a recent exact result shows that the average travel time evolves proportionally to the harmonic mean velocity for $x/l_y \to 0$ and to the arithmetic mean for $x/l_y \gg 1$ [*Dagan et al.*, 1992].

It is clear that all models yield a consistent picture for relatively homogeneous log conductivity fields. Although at increasing heterogeneity accounting for time-dependent dispersion coefficients via (9) improves the likelihood of the distribution, this effect is not major. We therefore conclude from the body of results that the linear asymptotic model (8) is a robust model of travel time distributions in our experimental range ($\sigma_Y^2 \leq 1.6$).

## 6. Conclusions

The following conclusions can be drawn from the present numerical study on dispersion in heterogeneous porous formations:

1. Nonlinearity affects velocity statistics. Covariance functions are significantly modified, in particular in proximity to the origin of the spatial lag. Cumulative frequencies from actual computations suggest that longitudinal velocities in heterogeneous (lognormal) transmissivity fields tend to be represented by nonnormal distributions at increasing heterogeneity. From our examination of spatial moments (up to fourth order), it seems that the distribution is somewhere between normality and lognormality. Transverse velocities retain a normal distribution characteristic of linear models. This has implications on theoretical closures of the nonlinear problem.

2. Accuracy and convergence of computations in the range $\sigma_Y^2 \leq 1.6$ require up to four generation points of log transmissivity per integral scale and 1500 MC realizations to stabilize averages of second moments of the displacement distributions. This has implications on the problem size for single-realization studies of the same type.

3. A comparison of numerical displacement variances with results of linear theories shows an unexpectedly broad validity field for the theoretical results. It is suggested that this may be due to opposite deviations from linear theoretical results induced by independent linearizations of flow and transport.

*Acknowledgments.* This paper is a spin-off of the project MURST 40% "Fenomeni di trasporto nel ciclo idrologico." The writers are deeply indebted to Prof. Gedeon Dagan, Tel Aviv University, for continuous advice and support and for crucial comments on early draft of this paper.

## References

Ababou, R., D. McLaughlin, L. W. Gelhar, and A. F. B. Tompson, Numerical simulation of three-dimensional saturated flow in randomly heterogeneous porous media, *Transp. Porous Media*, *4*, 549–565, 1989.

Barry, D. A., J. Coves, and G. Sposito, On the Dagan model of solute transport in groundwater: Application to the Borden site, *Water Resour. Res.*, *24*(10), 1805–1817, 1988.

Bellin, A., Sulla formulazione del trasporto in pezzi porosi eterogenei, paper presented at XXII Convegno di Idraulica e Costruzioni Idrauliche, Univ. della Calabria, Cosenza, Italy, 1990.

Bellin, A., Numerical generation of random fields with specified spatial correlation structure, *Tech. Rep. IDR 2/1991*, 53 pp., Dep. of Civ. Environ. Eng., Univ. of Trento, Trent, Italy, 1991.

Clifton, P. M., and S. P. Neuman, Effects of kriging and inverse modeling on conditional simulation of the Avra aquifer in southern Arizona, *Water Resour. Res.*, *18*(4), 1215–1234, 1982.

Dagan, G., Solute transport in heterogeneous porous formations, *J. Fluid Mech.*, *145*, 151–177, 1984.

Dagan, G., Theory of solute transport by groundwater, *Annu. Rev. Fluid Mech.*, *19*, 183–215, 1987.

Dagan, G., Time-dependent macrodispersion for solute transport in anisotropic heterogeneous aquifers, *Water Resour. Res.*, *24*(9), 1491–1500, 1988.

Dagan, G., *Flow and Transport in Porous Formations*, Springer-Verlag, New York, 1989.

Dagan, G., Transport in heterogeneous porous formations: Spatial moments, ergodicity and effective dispersion, *Water Resour. Res.*, *26*, 1281–1290, 1990.

Dagan, G., and V. Nguyen, A comparison of travel time concentration approaches to modelling transport by groundwater, *J. Contam. Hydrol.*, 4, 79–81, 1989.

Dagan, G., V. Cvetkovic, and A. M. Shapiro, A solute flux approach to transport in heterogeneous formations, 1, The general framework, *Water Resour. Res.*, *28*, 1369–1376, 1992.

Freeze, R. A., A stochastic-conceptual analysis of one-dimensional groundwater flow in nonuniform homogeneous media, *Water Resour. Res.*, *11*(5), 725–741, 1975.

Freyberg, D. L., A natural gradient experiment on solute transport in a sand aquifer, 2, Spatial moments and the advection and dispersion of nonreactive tracers, *Water Resour. Res.*, *22*(13), 2031–2046, 1986.

Gambolati, G., Fast solution to finite element flow equations by Newton iteration and modified conjugate gradient methods, *Int. J. Numer. Methods Eng.*, *15*, 661–675, 1980.

Gambolati, G., *Elementi di Calcolo Numerico*, Cortina, Padua, Italy, 1988.

Garabedian, S. P., D. R. Le Blanc, L. W. Gelhar, and M. A. Celia, Large scale natural gradient test in sand gravel, Cape Cod, Massachusetts, 2, Analysis of spatial moments for a nonreactive tracer, *Water Resour. Res.*, *27*(5), 911–924, 1991.

Gelhar, L. W., Stochastic subsurface hydrology from theory to applications, *Water Resour. Res.*, *22*(9), 135S–145S, 1986.

Gelhar, L. W., and C. L. Axness, Three-dimensional stochastic analysis of macrodispersion in aquifers, *Water Resour. Res.*, *19*(1), 161–180, 1983.

Graham, W. D., and D. B. McLaughlin, A stochastic model of solute transport in groundwater: Application to the Borden, Ontario, tracer test, *Water Resour. Res.*, *27*(6), 1345–1359, 1991.

Gutjahr, A. L., Fast Fourier transform for random field generation, project report, contract 4-RS of Los Alamos National Laboratory, N. M. Inst. of Min. and Technol., Socorro, 1989.

Johnson, C., *Numerical Solution of Partial Differential Equations by the Finite Element Method*, Cambridge University Press, New York, 1987.

Kraichnan, R. H., Diffusion by a random velocity field, *Phys. Fluids*, *13*, 22–31, 1970.

Le Blanc, D. R., S. P. Garabedian, K. M. Hess, L. W. Gelhar, R. D. Quadri, K. G. Stollenwerk, and W. W. Wood, Large-scale natural gradient test in sand and gravel, Cape Cod, Massachusetts, 1, Experimental design and observed tracer movement, *Water Resour. Res.*, *27*(5), 895–910, 1991.

Lundgren, T. S., and Y. B. Pointin, Turbulent self-diffusion, *Phys. Fluids*, *19*, 355–361, 1975.

Mackay, D. M., D. L. Freyberg, P. V. Roberts, and J. A. Cherry, A natural gradient experiment on solute transport in a sand aquifer, 1, Approach and overview of plume movement, *Water Resour. Res.*, *22*(13), 2017–2029, 1986.

Mantoglou, A., and J. L. Wilson, The turning bands method for the simulation of random field using line generation by a spectral method, *Water Resour. Res.*, *18*(5), 1379–1394, 1982.

Matheron G., and G. de Marsily, Is transport in porous media always diffusive? A counterexample, *Water Resour. Res.*, *16*(5), 901–917, 1980.

Naff, R. L., T. C. J. Yeh, and M. W. Kemblowski, A note on the recent natural gradient tracer test at the Borden site, *Water Resour. Res.*, *24*,(12), 2099–2103, 1988.

Neuman, S. P., and Y. K. Zhang, A quasi-linear theory of non-Fickian and Fickian subsurface dispersion, 1, Theoretical analysis with application to isotropic media, *Water Resour. Res.*, *26*(5), 887–902, 1990.

Neuman, S. P., C. L. Winter, and C. M. Newman, Stochastic theory of field-scale Fickian dispersion in anisotropic porous media, *Water Resour. Res.*, *23*(3), 453–466, 1987.

Øksendal, J., *Stochastic Differential Equations*, Springer-Verlag, New York, 1988.

Pinder, G. F., and W. G. Gray, *Finite Element Simulation in Surface and Subsurface Hydrology*, Academic, San Diego, Calif., 1977.

Rajaram, H., and L. W. Gelhar, Three-dimensional spatial moments analysis of the Borden tracer test, *Water Resour. Res.*, *27*(6), 1239–1251, 1991.

Rinaldo, A., A. Marani, and R. Rigon, Geomorphological dispersion, *Water Resour. Res.*, *27*(4), 513–525, 1991.

Rubin, Y., Stochastic modeling of macrodispersion in heterogeneous porous media, *Water Resour. Res.*, *26*(1), 133–141, 1990. (Correction, *Water Resour. Res.*, *26*(10), 2631, 1990.)

Rubin, Y., and G. Dagan, Stochastic analysis of boundaries effects on head spatial variability in heterogeneous aquifers, 1, Constant head boundary, *Water Resour. Res.*, *24*(10), 1689–1697, 1988.

Rubin, Y., and G. Dagan, Stochastic analysis of boundaries effects on head spatial variability in heterogeneous aquifers, 2, Impervious boundaries, *Water Resour. Res.*, *25*(4), 707–712, 1989.

Russo, D., Stochastic analysis of simulated vadose zone solute transport in a vertical cross section of heterogeneous soil during nonsteady water flow, *Water Resour. Res.*, *27*(3), 267–283, 1991.

Salandin P., Sulla dispersione di soluto in formazioni porose eterogenee, Ph.D. dissertation, 142 pp., Univ. of Padua, Padua, Italy, 1990.

Salandin, P., and A. Rinaldo, Numerical experiments on dispersion in heterogeneous porous media, in *Computational Methods in Subsurface Hydrology*, edited by G. Gambolati et al., pp. 495–501, Springer-Verlag, New York, 1990.

Salandin, P., A. Rinaldo, and G. Dagan, A note on transport in stratified formations by flow tilted with respect to the bedding, *Water Resour. Res.*, *27*, 3009–3017, 1991.

Shapiro, A. M., and D. Cvetkovic, Stochastic analysis of solute arrival time in heterogeneous porous media, *Water Resour. Res.*, *24*(10), 1711–1718, 1988.

Smith, L., and R. A. Freeze, Stochastic analysis of steady state groundwater flow in a bounded domain, 2, Two-dimensional simulations, *Water Resour. Res.*, *15*(6), 1543–1559, 1979.

Smith, L., and F. W. Schwartz, Mass transport, 1, A stochastic analysis of macrocopic dispersion, *Water Resour. Res.*, *16*(2), 303–313, 1980.

Smith, L., and F. W. Schwartz, Mass transport, 2, Analysis of uncertainty in prediction, *Water Resour. Res.*, *17*(2), 351–369, 1981.

Sudicky, E. A., A natural gradient experiment on solute transport in a sand aquifer: Spatial variability of hydraulic conductivity and its role in the dispersion process, *Water Resour. Res.*, *22*(13), 2069–2082, 1986.

Taylor, G. I., Diffusion by continuous movements, *Proc. London Math. Soc., Ser. A*, *20*, 196–212, 1921.

Tompson, A. F. B., and L. W. Gelhar, Numerical simulation of solute transport in three-dimensional, randomly heterogeneous porous media, *Water Resour. Res.*, *26*(10), 2541–2562, 1990.

Tompson, A. F. B., R. Ababou, and L. W. Gelhar, Implementation of the three-dimensional turning bands field generator, *Water Resour. Res.*, *25*(10), 2227–2243, 1989.

Valocchi, A. J., Numerical simulation of the transport of adsorbing solutes in heterogeneous aquifers, in *Computational Methods in Subsurface Hydrology*, edited by G. Gambolati et al., pp. 373–382, Springer-Verlag, New York, 1990.

Woodbury, A. D., and E. A. Sudicky, The geostatistical characteristics of the Borden aquifer, *Water Resour. Res.*, *27*(4), 533–546, 1991.

Zhang, Y. K., and S. P. Neuman, A quasi-linear theory of non-Fickian and Fickian subsurface dispersion, 2, Application to anisotropic media and the Borden site, *Water Resour. Res.*, *26*(5), 903–913, 1990.

A. Bellin and A. Rinaldo, Dipartimento di Ingegneria Civile ed Ambientale, Universitá di Trento, Mesiano di Povo, I-38050 Trento, Italy.

P. Salandin, Istituto di Idraulica "Giovanni Poleni," Universitá di Padova, via Loredan 20, I-35131 Padova, Italy.

(Received October 7, 1991;
revised February 25, 1992;
accepted March 6, 1992.)